

## 4-(9-Anthryl)aniline. 1. Intramolecular Charge-Transfer State Formation in Solution

Seonkyung Lee, Koji Arita,<sup>†</sup> and Okitsugu Kajimoto\*

Department of Chemistry, Graduate School of Science, Kyoto University, Kitashirakawa-Oiwakecho, Sakyo-ku, Kyoto 606-01, Japan

Kohei Tamao

The Chemical Research Institute of Kyoto University, Gokasyou, Uji, Kyoto 611, Japan

Received: January 24, 1997; In Final Form: May 15, 1997<sup>⊗</sup>

4-(9-Anthryl)aniline (AA) was synthesized for the first time, and its absorption and fluorescence spectra, as well as its fluorescence lifetime, were measured in various solvents. The absorption spectra of AA are nearly independent of the solvent polarity while the fluorescence spectra and its lifetimes are strongly dependent on the solvents. The dipole moment of the fluorescent state was evaluated to be 15.8 D in the solvent polarity range  $f(\epsilon, n) = 0.45 \sim 0.8$ . The large dipole moment, together with the largely red-shifted fluorescence and its long radiative lifetime, demonstrates the formation of the intramolecular charge-transfer state.

### 1. Introduction

Upon photoexcitation, a group of compounds called “twisted intramolecular charge-transfer (TICT)” molecules form the charge-transfer state whose donor and acceptor parts are perpendicular with each other. Such a TICT state is formed only in polar solvents such as alcohol, acetone, and acetonitrile.<sup>1–3</sup> These molecules attract renewed attention because of the recent development in the detailed analysis of internal rotation under supersonic jet conditions. We have studied the structure and dynamics of these compounds in a supersonic jet since 1986 and have reported the results for (*N,N*-dimethylamino)benzotrile,<sup>4,5</sup> 3,5-dimethyl-4-(*N,N*-dimethylamino)benzotrile,<sup>6</sup> 9,9'-bianthryl (BA),<sup>7–9</sup> and 4-(9-anthryl)dimethylaniline (ADMA).<sup>10</sup> The potential around the twisting angle was found to be quite important in determining the behavior of the TICT state formation.

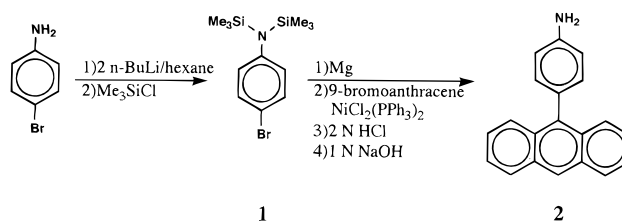
Among the molecules forming a TICT state in polar solvents, BA and ADMA are known to give a sharp contrast in their dynamic behavior of the TICT state formation. In the case of BA, the time dependence of the charge-transfer (CT) fluorescence can be analyzed simply in terms of the two-state model including only the locally excited (LE) and the CT states.<sup>11</sup> In contrast, for ADMA, the rise and decay curve of the CT fluorescence is known to be quite complex.<sup>12</sup> One has to assume many intermediate states between the LE and the CT states or use several lifetimes for the curve fitting. In addition, the transient absorption spectra cannot be expressed by a linear combination of the absorption of the LE and the CT states.<sup>13</sup> The reason for such a big difference between these two molecules, BA and ADMA, has not been fully analyzed yet though a large number of related data have been published. In this respect, determination of the torsional potential and the study of isolated solvated clusters of these compounds in a supersonic jet are important. Some years ago, we measured the laser-induced fluorescence (LIF) spectra of BA and determined the torsional potential. In the  $S_0$  state, two anthryl moieties are perpendicular with each other, while in the  $S_1$  state the equilibrium angle is  $68^\circ$ .<sup>7</sup> We also attempted to determine the

equilibrium torsional angle of ADMA, but found that the LIF spectra is much too congested to deduce the torsional potential.

In the present series of study, we have for the first time synthesized and studied 4-(9-anthryl)aniline (AA), which has the same structure as ADMA except for the methyl groups being substituted by hydrogen atoms. Because of the reduced number of internal rotors comparing with ADMA, AA is expected to show sharp separate peaks in its LIF excitation spectra, which help us to deduce detailed information about the torsional potential. We have first measured the absorption and fluorescence spectra together with the fluorescence lifetimes in several polar solvents to assure the CT state formation, then studied the structure and torsional potential of AA in a free jet, and finally observed the CT state formation of AA-polar molecule complexes in a free jet. This paper presents the first part of the study, the synthesis of AA and its CT state formation in solution.

### 2. Experimental Section

**2.1. Synthesis of 4-(9-Anthryl)aniline.** Since 4-(9-anthryl)aniline has been synthesized for the first time, the synthetic procedure will be given in detail. The total scheme of the synthesis was



*p*-Bromoaniline (8.61 g, 50 mmol) was reacted with *n*-BuLi (in hexane, 1.70 M, 62 mL, 105 mmol) in tetrahydrofuran (THF) for 2 h at  $-70^\circ\text{C}$  and subsequently with  $\text{Me}_3\text{SiCl}$  (14 mL, 110 mmol) for 0.5 h at the same temperature under nitrogen atmosphere. After being stirred for an additional 1 h at room temperature, the reaction mixture was filtrated and condensed under reduced pressure. Distillation from the mixture (89–91  $^\circ\text{C}/0.7$  mmHg) gave disilylated compound **1** in 68% yield (10.8 g, 34 mmol).

<sup>†</sup> Present address: Electronics Research Laboratory, Corporate Technology Center, Matsushita Electronics Corporation, Takatsuki, Osaka 569, Japan.

<sup>⊗</sup> Abstract published in *Advance ACS Abstracts*, June 15, 1997.

A Grignard reagent (0.37 M, 58 mL, 21.1 mmol) prepared from compound **1** and Mg in THF were added to a THF (50 mL) solution of 9-bromoanthracene (4.97 g, 19.3 mmol) and  $\text{NiCl}_2(\text{PPh}_3)_2$  (0.19 g, 0.3 mmol) at 0 °C under a nitrogen atmosphere. This mixture was refluxed for 1 h. After the confirmation of completion of the reaction by thin-layer chromatography, HCl (2 N, 90 mL) was added dropwise to the mixture at 0 °C, and the mixture was stirred for 0.5 h at room temperature. After extraction with ether, the organic layer was washed with 1 N NaOH several times and dried over  $\text{MgSO}_4$ . The resulting mixture was filtered and condensed under reduced pressure. Recrystallization from ethanol afforded 3.05 g (11 mmol) of 4-(9-anthryl)aniline in 57% yield as yellow crystals: mp 132–133 °C;  $^1\text{H NMR}$  ( $\text{CDCl}_3$ )  $\delta$  3.83 (brs, 2H), 6.86–6.94 (m, 2H), 7.16–7.24 (m, 2H), 7.28–7.49 (m, 4H), 7.73–7.81 (m, 2H), 7.98–8.06 (m, 2H), 8.45 (s, 1H);  $^{13}\text{C}$  ( $\text{CDCl}_3$ )  $\delta$  114.97, 125.00, 125.03, 126.07, 127.08, 128.27, 128.57, 130.60, 131.45, 132.15, 137.38, 145.66; MS *m/e* (relative intensity) 269 ( $\text{M}^+$ , 100). Anal. Calcd for  $\text{C}_{20}\text{H}_{15}\text{N}$  (269.346): C, 89.19; H, 5.61; N, 5.20. Found: C, 89.24; H, 5.57; N, 5.15.

**2.2. Absorption and Fluorescence Measurements.** Absorption spectra were taken with a Shimadzu UV-240 spectrophotometer. Fluorescence spectra were recorded with a Shimadzu RF-502A spectrofluorophotometer. Fluorescence grade hexane, cyclohexane, benzene, chloroform, dichloromethane, and acetonitrile and spectrograde ethanol were used without further purification. All solutions were deaerated by repeated freeze–pump–thaw cycles.

**2.3. Lifetime Measurements.** Fluorescence lifetimes were determined by the time-correlated single-photon counting method using a mode-locked Ti:sapphire laser (Spectra-Physics, Tsunami model 3950) which was pumped by a continuous wave argon ion laser (Spectra-Physics, Beamlock 2060). The laser pulse was frequency-doubled (383 nm) with a  $\text{LiIO}_3$  crystal and used for exciting the sample. The full width at half-maximum (fwhm) of the instrument response function for the laser system was about 100 ps.

Samples were placed in quartz tubes, deaerated, and sealed. A Hamamatsu R2809-02u microchannel plate photomultiplier tube was used for detection. Data were collected typically up to  $6 \times 10^3$  counts in the peak channel.

Fluorescence spectra were carefully measured before and after laser excitation, and it was confirmed for all solutions that no detectable photochemical decomposition occurred except chloroform and dichloromethane.

### 3. Results and Discussion

**3.1. Absorption Spectra.** The absorption spectra of AA taken in nonpolar hexane and polar acetonitrile are shown in Figure 1. The absorption spectrum of AA is almost the same as anthracene and ADMA with intense vibronic peaks due to the anthracene  $6_0''$  vibration.<sup>14</sup> It appears, therefore, that the excitation occurs into a locally excited state where the anthracene moiety is excited. The shift in the absorption maximum by solvent polarity is very small, i.e., ca. 1 nm between these solvents, indicating that the degree of stabilization by these solvents is similar in both the ground and excited states. Complete similarity of the absorption spectra in the vibronic structure and the wavelength between these nonpolar and polar solvents indicates that the absorption occurs in both cases to the same excited state.

The width of the absorption peak is worth discussing in relation to the torsional potential around the phenyl–anthryl bond. As shown in Figure 2, the fwhm of the absorption peak is smaller for BA than for ADMA and AA. As demonstrated

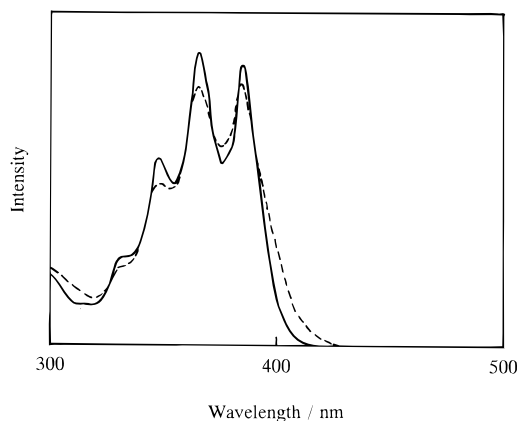


**Figure 1.** Absorption spectra of AA in hexane (—) and acetonitrile (---).

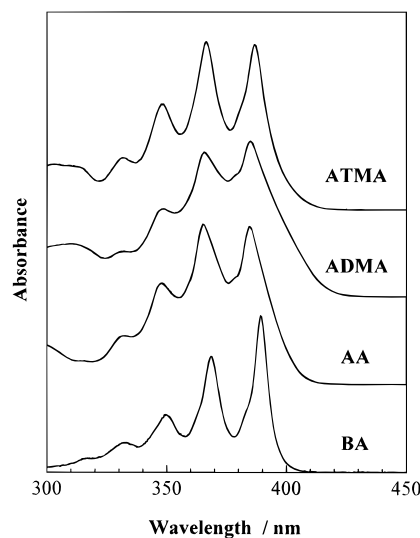


**Figure 2.** Absorption spectra of BA, AA, ADMA, and ATMA in cyclohexane, showing that the peak width is related to the molecular flexibility in the torsional motion.

by Wortmann et al.,<sup>15</sup> the shape of the absorption spectrum strongly reflects the torsional potential of BA both in the ground and excited states. In the case of BA, the ground state torsional potential has a very narrow valley around 90° (perpendicular orientation) because of the large repulsive force between the bulky anthryl moieties. The Franck–Condon region of the excited state is therefore narrow, and the absorption spectrum becomes sharp. In addition, the depth of the double-minimum torsional potential in the excited state is known to be small, which limits the energy range of the excitation from the ground state.

In contrast, the repulsive force between the aniline and anthracene moieties in AA and ADMA is rather small compared with the force between the two anthryl moieties of BA. This makes the torsional motion more flexible, and the potential curve around 90 degrees becomes much flatter, or even makes the equilibrium position deviate from the perpendicular position in the ground state. Consequently, the Franck–Condon region in the excited state becomes much wider and thus the peak width of the absorption spectrum also becomes wider. If one attaches methyl substituents to the 3,5-positions of benzene ring to limit the flexibility in the torsional motion, the absorption peak again gets sharper as demonstrated by the spectrum of 4-(9-anthryl)-3,5-dimethyl-*N,N*-dimethylaniline (ATMA). In this way we can infer the flatness of the torsional potential in the cases of ADMA and AA from the observed broadness of the absorption spectrum. Such a difference in the flexibility of torsional motion strongly

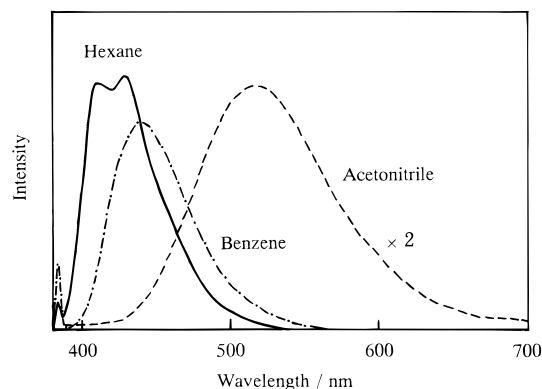


**Figure 3.** Fluorescence spectra of AA in various solvents: [AA] =  $1.0 \times 10^{-5}$  M at room temperature.

affects the distribution of the torsional angle of BA or AA molecules in solution and eventually causes a significant difference in the dynamic behavior of the electron-transfer reaction.

**3.2. Dispersed Fluorescence Spectra and the CT State Formation in Polar Solvents.** The dispersed fluorescence spectra in various solvents are shown in Figure 3. The spectrum in nonpolar hexane shows a vibronic structure. In polar acetonitrile, however, the spectrum is devoid of vibronic structure and largely red-shifted. Among the solvents studied, the vibronic structure was observed in hexane and cyclohexane, whereas only the red-shifted structureless fluorescence was detected in benzene, chloroform, dichloromethane, ethanol, and acetonitrile. Two noticeable features in these fluorescence spectra of AA are worth discussing. First, the drastic change in the shape of the fluorescence spectra in polar solvents indicates that the fluorescent state is completely different from the originally excited LE state. Second, the increasing Stokes' red shift with increasing solvent polarity implies that AA in the fluorescent state has a large dipole moment. This fluorescent state, possessing a large dipole moment, is most likely the intramolecular charge transfer state. One can conclude from the results of the absorption and the fluorescence experiments that AA is first excited to the LE state and then, if it is in polar media, transfers to the CT state.

The difference in the fluorescence maximum between non-polar hexane and polar acetonitrile was about  $5000 \text{ cm}^{-1}$  for AA, while in ADMA, the difference was  $7000 \text{ cm}^{-1}$ . This fact suggests that the dipole moment of ADMA is larger than that of AA. In order to estimate the dipole moment of the CT state, the fluorescence band maxima are plotted in Figure 4 against solvent polarity parameters according to the Lippert–Mataga equation.<sup>16</sup>

$$\nu_{\text{CT}} = \nu_{\text{CT}}(0) - \frac{\mu_{\text{e}}^2}{hca^3} f(\epsilon, n) \quad (1)$$

with

$$f(\epsilon, n) = \frac{2(\epsilon - 1)}{(2\epsilon + 1)} - \frac{(n^2 - 1)}{(2n^2 + 1)} \quad (2)$$

where  $\nu_{\text{CT}}$  and  $\nu_{\text{CT}}(0)$  denote the emission maximum of each solution and the hypothetical gas-phase emission maximum in wavenumbers,  $\mu_{\text{e}}$  is the excited state dipole moment,  $a$  is the Onsager radius of the solute, and  $\epsilon$  and  $n$  are the dielectric constant and the refractive index of the solvent, respectively. The dipole moment of the CT state can be estimated from the slope of the straight line in the region of higher solvent polarity,

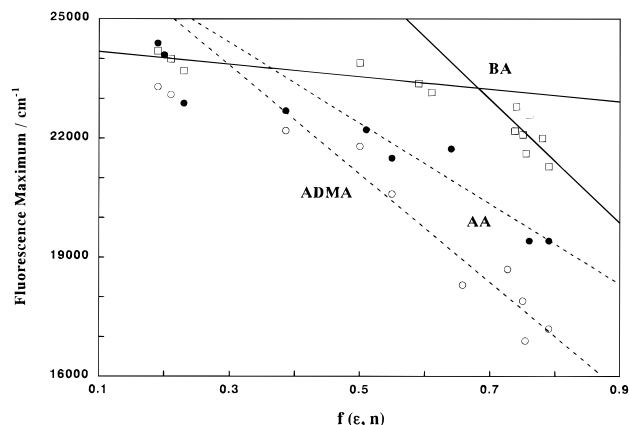


**Figure 4.** Solvent effects on the fluorescence band maxima ( $\nu_{\text{max}}$ ) of AA (●), ADMA (○), and BA (□). The solvent parameter is  $f(\epsilon, n) = \{2(\epsilon - 1)/(2\epsilon + 1) - (n^2 - 1)/(2n^2 + 1)\}$ , where  $\epsilon$  and  $n$  are the dielectric constant and refractive index of the solvent, respectively.

though the points are rather scattered. By the straight-line analyses of the plots in the range  $f(\epsilon, n) = 0.45 \sim 0.8$ , the dipole moment was evaluated to be about 18.4 and 15.8 D for ADMA and AA, respectively, taking the cavity radius in Onsager's reaction field theory as 5 Å. The smaller dipole moment observed for AA is due to the smaller electron-donating power of the amino group compared with the dimethylamino substituent in ADMA.

**3.3. Energy Level of the CT State: Comparison between BA and AA.** Although we use the Lippert–Mataga equation to estimate the excited state dipole moment, it is important to realize that the equation is not appropriate when the nature of the excited state changes gradually from an LE-like state to a TICT-like state with increasing polarity of solvents. Similar to the trend reported for ADMA, the plot for AA cannot be represented by a single straight line but is curved or represented by the superposition of several lines of different slopes. The convex shape in the plot suggests that the charge-transfer character of the emitting state, and hence the dipole moment, increases with increasing solvent polarity.

The value  $\nu_{\text{CT}}(0)$ , i.e., the hypothetical CT fluorescence maximum in the gas phase, can be obtained from the (ordinate) intercept of the plot in Figure 4, though it contains some uncertainty. Then, one can roughly estimate the energy gap between the LE and the CT states of an isolated molecule. For AA, the hypothetical emission maximum obtained from the plot is about  $27400 \text{ cm}^{-1}$ . Using the observed absorption maximum of  $26100 \text{ cm}^{-1}$ , the energy gap is estimated to be about  $1300 \text{ cm}^{-1}$ ; the CT state is only slightly higher in energy than the LE state. Such a small gap may facilitate the mixing of these two states even in a nonpolar solvent. Interestingly, in Figure 2, all three compounds having an amino group exhibit the long tail toward longer wavelength, suggesting the possible appearance of the CT state beneath the strong LE absorption even in nonpolar cyclohexane.

On the other hand, for BA, the CT state of an isolated molecule is known to have a higher energy compared to that in AA and ADMA. Actually, from the plot for BA in Figure 4, one can obtain the energy gap of about  $8200 \text{ cm}^{-1}$  using the intercepts of the two separate lines for the LE and the CT states. It is quite likely that the difference in the energy gap between AA and BA plays an important role for the drastic difference of the dynamic behavior in the CT state formation. However, such a low-lying CT state has not been observed in the solution phase. This is probably due to the small transition moment to the CT state and also due to the broad absorption spectra which makes the discrimination between the two transitions difficult.

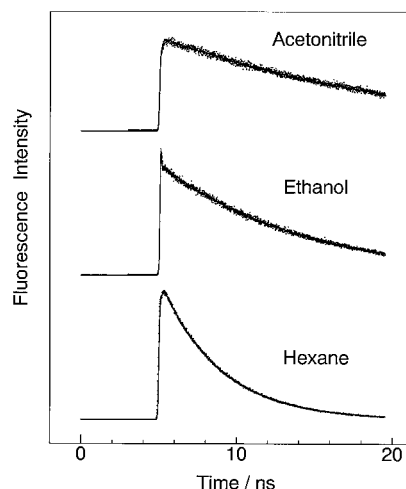


**Figure 5.** Fluorescence decay curves monitored at the fluorescence maxima of AA in various solvents excited at 383 nm.

In order to unambiguously show the presence of such a CT state, the detailed spectroscopic observation of an isolated molecule in a free jet and its analysis in terms of the electronic structure and torsional potential must be necessary.

**3.4. Lifetimes of the LE and the CT States.** The solutions of AA in various solvents were excited with picosecond laser pulses at 383 nm. The fluorescence rise and decay curves were measured at selected emission wavelengths. The rise time at the fluorescence maximum in polar solvents was too rapid to deduce the rate of electron transfer; the electron-transfer reaction was completed within 20 ps. Typical decay curves observed at the fluorescence maximum are shown in Figure 5. The emission at shorter wavelength (ca. 410 nm) mainly originates from the LE form whereas the emission at longer wavelength comes from the CT state. All the observed decay curves were well fitted by single-exponential functions. The decay curve in nonpolar hexane gave a lifetime of 3.2 ns, while that in polar acetonitrile was 13.2 ns. In chloroform and dichloromethane, fluorescence spectra changed with time of exposure to picosecond laser pulses, though it did not show any significant change by repeated measurements with an ordinary fluorometer. AA seems to react slowly with chloroform and dichloromethane upon irradiation by intense laser pulses. For chloroform, the measurement was carried out within a short period where the change due to the slow reaction can be neglected.

The decay curve of AA in ethanol measured at its fluorescence maximum has two components: a fast decay component with a lifetime of 40 ps and a slow decay component with a lifetime of 7.6 ns. The reason for the presence of the fast decay component is not certain at this stage. However, such a fast decay component was also observed by Anthon et al. for BA in alcohol solutions<sup>17</sup> and by Siemiarz and Ware for ADMA in 2-propanol.<sup>13</sup> Since the fast component of the fluorescence decay is only seen in hydrogen-bonding solvent, some process including excited-state hydrogen bonding may be responsible for this fast decay. The lifetimes in various solvents are listed in Table 1.

One can see from Table 1 that the lifetime increases with increasing solvent polarity. This trend is in agreement with the previous results for ADMA and substituted anthracenes; Table 2 compares the lifetimes of the fluorescent states among AA, ADMA, and BA in typical nonpolar and polar solvents. Generally, the lifetime of the CT state is longer than that of the LE state and becomes further longer with increasing solvent

**TABLE 1: Fluorescence Lifetimes of AA in Various Solvents**

solvent	$\nu_{\max}$ , $10^3 \text{ cm}^{-1}$	lifetime, ns
<i>n</i> -hexane	24.4	3.2
cyclohexane	24.1	3.2
chloroform	22.2	(4)
dichloromethane	21.7	
ethanol	19.4	7.6
acetonitrile	19.4	13.2

**TABLE 2: Comparison of the Fluorescence Lifetimes (ns) among AA, ADMA, and BA**

solvent	AA	ADMA <sup>a</sup>	BA <sup>b</sup>
<i>n</i> -hexane	3.2	2.1	8
ethanol	7.6		33
acetonitrile	13.2	31.4	35

<sup>a</sup> Values taken from ref 14. <sup>b</sup> Values taken from ref 20.

polarity.<sup>18,19</sup> The polarity dependence in the lifetime of AA is in accord with the above tendency and therefore supports the formation of the CT state in polar solvent.

In conclusion, the above mentioned three types of features of the fluorescent state in polar solvents—large dipole moment, largely red-shifted fluorescence, and its long radiative lifetime—confirm that 4-(9-anthryl)aniline forms the intramolecular charge-transfer state in polar solvent. In addition, from the width of the absorption spectrum and the trend in the solvatochromic fluorescence shift, the characteristics of AA are quite similar to that of ADMA.

**Acknowledgment.** This work is partially supported by the Grani-in-Aid (number 06453022) from the Ministry of Education, Science and Culture.

## References and Notes

- Grabowski, Z. R.; Rotkiewicz, K.; Siemiarz, A.; Cowley, D. J.; Baumann, W. *Nouv. J. Chim.* **1979**, *3*, 443.
- Rettig, W.; Zander, M. *Ber. Bunsen-Ges. Phys. Chem.* **1983**, *87*, 1143.
- Rettig, W.; Chandross, E. A. *J. Am. Chem. Soc.* **1985**, *107*, 5617.
- Kobayashi, T.; Futakami, M.; Kajimoto, O. *Chem. Phys. Lett.* **1986**, *130*, 63.
- Yokoyama, H.; Kajimoto, O.; Ooshima, Y.; Endo, Y. *Chem. Phys. Lett.* **1991**, *179*, 455.
- Kobayashi, T.; Futakami, M.; Kajimoto, O. *Chem. Phys. Lett.* **1987**, *141*, 450.
- Yamasaki, K.; Arita, K.; Kajimoto, O.; Hara, K. *Chem. Phys. Lett.* **1986**, *123*, 277.
- Kajimoto, O.; Yamasaki, K.; Arita, K.; Hara, K. *Chem. Phys. Lett.* **1986**, *125*, 184.
- Honma, K.; Arita, K.; Yamasaki, K.; Kajimoto, O. *J. Chem. Phys.* **1991**, *94*, 3496.
- Kajimoto, O.; Hayami, S.; Shizuka, H. *Chem. Phys. Lett.* **1991**, *177*, 219.
- Kang, T. J.; Kahlow, M. A.; Giser, D.; Swallen, S.; Nagarajan, V.; Jarzaba, W.; Barbara, P. F. *J. Phys. Chem.* **1988**, *92*, 6800.
- Siemiarz, A.; Ware, W. R. *J. Phys. Chem.* **1987**, *91*, 3677.
- Okada, T.; Mataga, N.; Baumann, W.; Siemiarz, A. *J. Phys. Chem.* **1987**, *91*, 4490.
- (a) Okada, T.; Fujita, T.; Mataga, N. *Z. Phys. Chem. N. F.* **1976**, *101*, 57. (b) Okada, T.; Fujita, T.; Kubota, M.; Masaki, S.; Mataga, N.; Ide, R.; Sakata, Y.; Misumi, S. *Chem. Phys. Lett.* **1972**, *14*, 563.
- Wortmann, R.; Elich, K.; Lebus, S.; Liptay, W. *J. Chem. Phys.* **1991**, *95*, 6371.
- (a) Mataga, N.; Kaifu, Y.; Koizumi, M. *Bull. Chem. Soc. Jpn.* **1955**, *28*, 690. (b) Pasman, P.; Rob, F.; Verhoeven, J. W. *J. Am. Chem. Soc.* **1982**, *104*, 5127.
- Anthon, D. W.; Clark, J. H. *J. Phys. Chem.* **1987**, *91*, 3530.
- Herbich, J.; Kapturkiewicz, A. *Chem. Phys.* **1993**, *170*, 221.
- Wang, S.; Cai, J.; Sadygov, R.; Lim, E. C. *J. Phys. Chem.* **1995**, *99*, 7416.
- Nakagima, N.; Murakawa, M.; Mataga, N. *Bull. Chem. Soc. Jpn.* **1976**, *49*, 854.